

The level crossing method and recent achievements of high-resolution laser spectroscopy

V. N. Grigor'eva, É. I. Ivanov, and N. I. Kaliteevskii

Leningrad State University
Usp. Fiz. Nauk **119**, 149-167 (May 1976)

The level crossing method is compared with current methods of laser spectroscopy. The compared methods supplement one another in the solution of certain problems of atomic physics and are based on quite different physical phenomena. The level crossing method is one of the simplest and most effective methods for investigating the structures of atomic levels. It makes it possible to measure the separations of very close atomic states that could not be resolved by classical spectroscopic methods. This is due to the fact that the crossing signal is determined by the characteristics of the emitting state and is not masked by the Doppler broadening that usually limits the spectroscopic resolution of close lines. For the same reasons, however, the method does not permit one to investigate phenomena associated with the line shape. Special laser-spectroscopy procedures have recently been developed (two-photon excitation and saturated absorption spectroscopy) in which the resolving power is determined, as in the crossing method, by the natural line width, and not by the Doppler width. This has made it possible in certain cases to achieve high resolution of spectral components and to investigate phenomena taking place "under cover" of the Doppler broadened line.

PACS numbers: 07.45.+r, 42.60.Qm, 32.10.Ks, 32.10.Nw

CONTENTS

1. Introduction	429
2. Current Level of Research by the Level-Crossing Method	429
3. High Resolution Laser Spectroscopy	433
4. Conclusion	438
References	438

1. INTRODUCTION

By now, methods involving the interference of atomic states have been widely developed,^[1] the level crossing method being the one most frequently used to determine atomic and nuclear parameters. This method makes it possible to measure extremely small separations of atomic levels that could not be resolved by classical spectroscopic methods.^[2] This is associated with the fact that the interference phenomena are determined by the characteristics of the emitting state and are not affected by Doppler broadening, which usually limits the spectroscopic resolution achievable in separating two close-lying lines. On the other hand, for the same reasons the method cannot be used to investigate phenomena involving line shapes (e.g., Bennett dips) nor to determine isotopic shifts.

Thus, the methods of optical spectroscopy were more universal but less precise than the level crossing method. Recently, however, special methods of laser spectroscopy have been developed (two-photon excitation, saturation spectroscopy) in which, as in the level crossing method, the limiting resolution is not determined by the Doppler broadening, but by the natural line width. This has made it possible in some cases to achieve a very high resolution of spectral components and to investigate phenomena taking place "under cover" of the Doppler line. It is accordingly of interest to compare

the level crossing method with modern methods of laser spectroscopy; these methods supplement one another in the solution of certain problems of atomic physics and are based on essentially different physical phenomena. The discussion of the level crossing method will be conducted mainly through examples taken from studies carried through in recent years at the Coherent-Optics Laboratory of the Physical Institute at Leningrad University. In reviewing the most recent achievements of laser spectroscopy, the original papers have been used, as well as communications presented by several research groups at the Fourth International Conference on Atomic Physics (Heidelberg, 1974).^[3] We shall not emphasize the theoretical study of physical phenomena, which has been described in detail in monographs^[4,4] and reviews,^[5,6] but shall devote most of our attention to a discussion of the spectroscopic applications.

2. CURRENT LEVEL OF RESEARCH BY THE LEVEL-CROSSING METHOD

Let us briefly recall the idea of the method. An external magnetic (electric) field lifts the degeneracy, splitting the level into magnetic sublevels, and if the levels are coherently excited, this results in depolarization of the fluorescence—the Hanle effect (the phenomenon of crossing at zero field). In the presence of hyperfine (fine) structure, the external field not only lifts the degen-

eracy at $H=0$, but also leads to the appearance of new degenerate states (crossing of levels), and this is accompanied by interference phenomena.

The widths of the Hanle and crossing signals bear information on the coherence time of the states (in the limiting case this is equal to the radiative decay time) and also depend (in a magnetic field) on the Landé g factors and (in an electric field) on the Stark constant β_j , which determine the splitting of the magnetic sublevels. The broadening of the signal with increasing pressure of the investigated or buffer gas provides a means for investigating the cross sections for atomic collisions that lead to additional depolarization of the radiation. The magnetic field strengths at which the levels cross are determined by the hyperfine structure (HFS) constants for the magnetic dipole (A) and electric quadrupole (B) interactions, as well as by the Landé factors. In addition to depending on A and B , the crossing position in an electric field also depends on the Stark constant β_j . Thus, the constants A and B (when g_j and g_I are known), the Stark constant β_j , as well as the lifetime τ and the cross sections for depolarizing collisions can be evaluated from an analysis of the crossing signals. A detailed study of the accidental and systematic errors inherent in the method has shown that such determinations can be made with high accuracy.^[7] The constants mentioned above are comparatively easy to determine for states for which the splitting of the hyperfine sublevels is large as compared with the natural width. When the HFS is narrow the crossings in nonzero fields are not resolved; then the experimental curve has a complex shape and the positions and widths of the crossing signals can only be determined by resolving the curve into components. Resolving the curve involves difficulties and may introduce additional errors.

The best way to process complex level crossing signals is to compare the experimental results with a quantum mechanical calculation in which account is taken of the changes in the energies of the Zeeman sublevels, in the probability amplitudes of the transitions, and in the coherence, as the applied external fields are altered. This method is being used successfully in our laboratory.

A detailed description of the application of the level crossing method to the determination of atomic constants has been given in a review article^[2] in which sodium and cesium atoms were used as examples. Here we shall discuss the determination of the atomic constants of rubidium by the level crossing method under the simultaneous action of external magnetic and electric fields. This question was not discussed in the review article cited above.

As we mentioned above, the level splitting in an electric field depends on the Stark constant β_j , and this constant can be determined by analyzing the crossing signals. In this case, however, the levels cross only in strong fields, the production of which involves definite experimental difficulties. In addition, the experimental results are difficult to interpret: the electric field not only splits the levels, but also shifts the

center of gravity of the term, and consequently shifts the absorption line with respect to the line used for excitation. The observed dependence of the intensity on the electric field strength is therefore due not only to the interference effects, but also to a change in the absorption of the exciting light.

The Stark constant of the $6^2P_{3/2}$ term of rubidium was therefore determined in^[8,9] under the simultaneous action of parallel electric and magnetic fields on the atoms. Even comparatively weak fields (2–3 kV/cm) considerably alter the interference signals, not only shifting the crossing signals on the magnetic-field scale, but also deforming the entire depolarization curve. The interference signals are seen against a background that increases monotonically with increasing magnetic field strength and arises from the dependence on the magnetic field strength of the transition probabilities, and hence of the part of the intensity due to incoherent scattering. The electric field also alters the transition probabilities, the changes in this case being dependent on β_j ; hence the entire curve turns out to be sensitive to the value of the Stark constant.

Figure 1 is a block diagram of the experimental setup. Resonance cells containing internal electrodes to produce the electric field were employed. The cell was mounted at the center of a pair of Helmholtz coils, which produced an adjustable magnetic field. The components of the laboratory field were compensated by additional coils. In the experiments on rubidium fluorescence, the illumination direction, the observation direction, and the direction of the applied fields were mutually perpendicular. The light source was an electrodeless lamp of the Bell-Bloom type. The exciting light was linearly polarized and coherently populated the $\Delta m_F = \pm 2$ magnetic sublevels. With this geometry, the interference signals have a Lorentz profile. The fluorescence passed through a rotating polaroid and fell onto a photomultiplier; the alternating component of the photocurrent, which is proportional to the intensity difference between two orthogonal polarizations, was registered with a phase sensitive detector.

Depolarization curves (Fig. 2) were recorded pointwise for different values of the magnetic field strength (at a fixed value of the electric field strength). The Stark constant was determined by comparing the experimental signals with calculated ones (the parameter

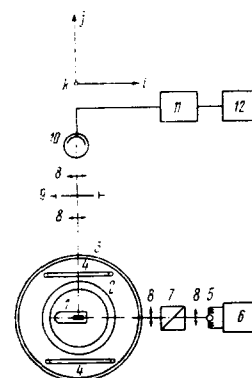


FIG. 1. Block diagram of apparatus for observing crossing signals in magnetic and electric fields. 1—resonance cell with internal electrodes, 2—Helmholtz coils, 3, 4—compensating coils, 5—Bell-Bloom rubidium lamp, 6—high frequency oscillator, 7—polarizing prism, 8—lenses, 9—rotating polaroid, 10—photomultiplier, 11—phase sensitive detector, 12—recorder.

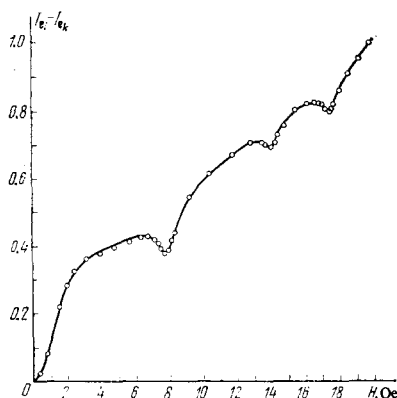


FIG. 2. Experimental curve (circles) obtained in a 2.125 kV/cm electric field, and the best-fit theoretical curve calculated with the parameter values $A = 8.16$ MHz, $B = 8.20$ MHz, $\tau = 97$ nsec, and $\beta_j = 0.260$ MHz/(kV/cm)².

values $A = 8.16 \pm 0.01$ MHz, $B = 8.20 \pm 0.010$ MHz, and $\tau = 97 \pm 3$ nsec were found by analyzing the crossing signals in a magnetic field^[10]. The theoretical curves were calculated on a computer, account being taken of the presence of two hyperfine components of different intensities in the exciting light (the splitting of the $5^2S_{1/2}$ ground state of Rb⁸⁵ amounts to 3036 MHz). In calculating the theoretical curves, the Stark constant β_j was varied so as to obtain a theoretical curve (and consequently a value of β_j) that agreed best with a given experimental curve. The value of β_j obtained this way from 12 experimental curves is 0.260 ± 0.007 MHz/(kV/cm)². The indicated error characterizes the reproducibility of the experimental results and illustrates what was said above about the high precision of the level crossing method. The systematic error in determining the Stark constant by this method is composed mainly of a 2.2% error due to the error in measuring the electric field strength (this error is composed of a 0.5% error in measuring the applied potential, a 0.1% error in measuring the distance between the electrodes, and a 0.5% error due to the nonuniformity of the electric field; the resulting 1.1% error becomes an error of 2.2% in β_j because the latter is quadratic in the electric field strength), a 1% error due to the nonlinearity of the recording system, a 0.17% calibration error, a 0.07% error due to nonuniformity of the magnetic field, and a 0.12% alignment error; the over-all systematic error is accordingly about 4% or 0.01 MHz/(kV/cm)².

Until recently, the level crossing method had been used in studying alkali metal atoms only for investigating the first 2P states. This is due to the fact that only these states can be directly populated with adequate efficiency by optical excitation since the $^2S \rightarrow ^2P$ transition probabilities fall off rapidly with increasing energy of the P level and the usual optical excitation sources are not efficient enough. In individual cases 2S and 2D states have been populated by cascade transitions from 2P states, but this mechanism for populating 2S and 2D levels is limited to the very lowest states. There have been individual experiments in which an electron beam was used to excite high-lying states.^[12] Electron beam excitation, however, is complicated by a number of

technical difficulties; moreover, such excitation is not very selective. The coincidence of the $\lambda = 388.865$ nm helium line with one of the hyperfine components of the $8^2P_{1/2} - 6^2S_{1/2}$ ($F = 4$) Cs transition was used in^[13] to populate the $8^2P_{1/2}$ Cs state by the light of a helium lamp and to observe the corresponding crossing signal at zero field.

Laser light can be used very effectively to excite certain high-lying atomic states. For example, the depolarization of the spontaneous emission from certain Ne levels excited by laser light has been used in our laboratory to determine the lifetimes of these high-lying levels. Below, we shall also describe experiments on the excitation of cadmium levels by the light from a pulsed laser whose active medium was cadmium vapor. However, the validity of such measurements requires more detailed discussion, to which we now turn.

The first observations of the depolarization of the spontaneous emission from a gaseous laser in longitudinal magnetic field were described in three independent papers.^[14-16] The widths of the Hanle signals were determined in the experiments for fixed values of the parameters of the medium and intensity of the laser light. However, it is difficult to analyze the signals to obtain the lifetimes and the cross sections for depolarizing collisions. The trouble is that laser light of comparatively high intensity must be used in order to obtain a sufficiently strong interference signal. Complicated nonlinear processes therefore take place, and one result of these is that the crossing signal for the spontaneous emission from one of the levels bears characteristics of the other state associated with the investigated stimulated emission. Transfer of coherence from other levels associated with the investigated spontaneous transitions also plays a definite part.

Owing to the presence of comparatively intense laser light, the weak-field approximation corresponding to second order perturbation theory is not entirely adequate, so terms up to the fourth order were included in the theoretical calculation of the signals. In most cases such a calculation leads to satisfactory agreement between theory and experiment, but some observed effects have not yet found their explanation.^[17]

The method has been used in our laboratory to investigate the spontaneous emission from neon-helium lasers generating in the visible at $0.63 \mu\text{m}$ and in the infrared at 1.15 and $3.39 \mu\text{m}$.^[18,19] An axial magnetic field, produced by Helmholtz coils, was applied to the investigated part of the discharge. The spontaneous emission, polarized perpendicular to the magnetic field, was observed through the wall of the discharge tube. The required spectrum line was isolated with a monochromator. To record the crossing signal, which amounted to only a small fraction of the light incident on the photodetector, the generation was modulated at low frequency and a phase sensitive detector was used to register only the alternating part of the photocurrent. The lifetimes of the corresponding levels and the cross sections for depolarizing collisions could be determined from the width of the recorded signals after extrapolation to zero

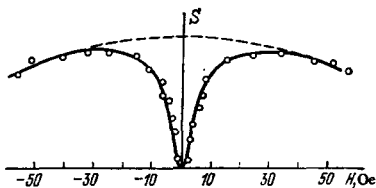


FIG. 3. Intensity of the 359.3 nm line vs magnetic field strength.

pressure and zero field power. As an example, the crossing signal from the $3p_4$ level of neon is shown in Fig. 3 against the background of the Doppler width, which is relatively small in the infrared region. By extrapolating the width of the Hanle signals to zero pressure, data could be obtained on the cross sections for depolarizing collisions and lifetimes for virtually all the active Ne levels.^[2]

The level crossing effect at zero field has recently been successfully observed with pulsed metal-vapor lasers.^[20,21] Apparatus consisting of a cadmium-vapor laser, an optical cell for observation, and a system for separating and recording the crossing signals, was assembled for the experiment.

The cadmium-vapor laser had a number of strong pulsed lasing modes in the afterglow (at 1.912, 1.648, 1.398, and 1.433 μm). The duration of the lasing action, measured at half height, was 50–70 μsec . The leading edge of the lasing pulse was delayed by 40–50 μsec with respect to the current pulse. A quartz prism was mounted within the resonator containing the active medium so that the light from any signal lasing mode could be extracted. The spontaneous emission was observed through the side walls of the cell in two mutually perpendicular directions. A continuous discharge in a mixture of cadmium vapor and a buffer gas was maintained in the cell. The interference signal amounted to only a small fraction (from 5×10^{-6} to 5×10^{-3}) of the total intensity of the observed line. The duty factor for the pulses was 0.025. A recording technique based on amplitude coding of the signal and subsequent accumulation was used to observe the small intensity changes. All the results were processed on a computer.

The theoretical calculations for the interpretation of the results were made, as in the case of the continuous laser, in the fourth order of perturbation theory, taking into account the nonlinear effects associated with the high intensity of the laser field, which in this case is especially important since brief but extremely strong excitation takes place in the pulsed laser. As a result of this, all the effects discussed above manifest themselves here in full force. Thus, for example, Fig. 4 shows the results of measurements of the crossing signal for the $5^3D_3-5^3P_2$ transition in cadmium, which illustrates the effect, mentioned above, of the mixing of the two interacting levels.

The results of calculating the crossing signal to fourth order terms in the field strength show that the curve can be resolved into two Lorentz curves whose widths are due to the Hertzian coherence times of the

upper and lower laser levels generating at 1.648 μm . Resolution of the contour into two components with widths γ_a and γ_b makes it possible to determine the lifetimes and the cross sections for depolarizing collisions for the 5^3D_3 and $4^3F_{2,3,4}$ levels of cadmium. The latter are in good agreement with published data obtained by different methods; this shows that the approximations made in the study and in performing the extrapolations are correct.^[21]

The highly excited states investigated in the studies enumerated above are laser levels, and of course there is only a limited number of such levels. It would seem promising to investigate the alignment of atoms in a discharge,^[22,23] in which the Hanle effect could be investigated for many high-lying levels; here, however, we cannot give a detailed discussion of this technique, which was proposed by Chaika^[24] and has been developed in recent years. The group of states that could be investigated would obviously be considerably enlarged if one should use a frequency-adjustable exciting source capable of populating any level that might be considered by optical means. A tuneable laser is such a source.

By now several studies have been published^[25,26] in which dye lasers have been used to achieve two-stage excitation of high-lying S, D, and F levels in Cs and Rb atoms, and crossing and double resonance signals from these levels have been observed. The experiment is performed as follows: A scattering cell containing an alkali metal is placed in a magnetic field. In the first stage of the excitation, the resonance light from a powerful lamp lit by a high frequency oscillator falls on the cell in the direction of the magnetic field and excites the atoms to the first 2P state. Then the atoms are brought to high-lying 2S and 2D states by means of a laser beam directed perpendicular to the external magnetic field and tuned to the frequency of the desired transition. The sequence of 2D states with principal quantum numbers $n=8-14$ and $^2S_{1/2}$ states with $n=9, 10, 11$ of Cs, as well as the 2D states with $n=6, 7, 8$ and $^2S_{1/2}$ states with $n=8, 9$ of Rb⁸⁷, have been successfully populated using rhodamine-6G and rhodamine-110 dye lasers pumped with an argon laser. It is interesting that the absorption of radiation at the resonance transi-

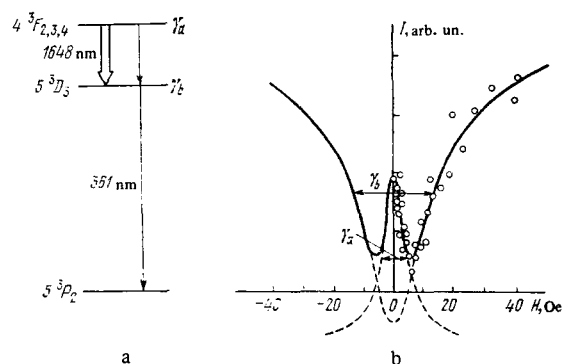


FIG. 4. Level scheme for cadmium (a), and the experimental crossing signal for the $5^3D_3-5^3P_2$ transition (circles) with resolution of the contour into two components (b).

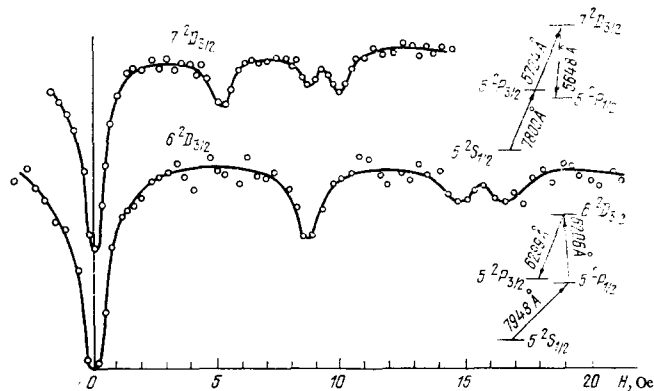


FIG. 5. Level crossing signals for the Rb^{87} $6^2D_{3/2}$ and $7^2D_{3/2}$ states.

tion plays a positive part in the two-stage excitation process—it increases the population of the first excited state.

All of the $^2D_{3/2}$ states have been investigated by the level crossing method and the values of their HFS constants have been determined or estimated. Figure 5 shows a recording of the crossing signals from Rb^{87} for the $6^2D_{3/2}$ and $7^2D_{3/2}$ states. The values of A and B found from the positions of the signals are as follows:

$$6^2D_{3/2}: |A| = 7.72(20) \text{ MHz}, |B| = 0.6(4) \text{ MHz} (B/A > 0),$$

$$7^2D_{3/2}: |A| = 4.55(15) \text{ MHz}, |B| = 0.36(18) \text{ MHz} (B/A > 0).$$

It may be assumed that when this method of investigating high-lying levels is further developed, it will be possible to determine the atomic constants characteristic of the above described applications of the level crossing method with high accuracy. It should be emphasized that requirements on the width of the exciting line from the tuneable laser play no important part in studies of atomic levels by the crossing method.

3. HIGH RESOLUTION LASER SPECTROSCOPY

The term *laser spectroscopy* is frequently used to denote extremely varied phenomena. In this review we shall use the term to denote all the methods of investigating the spectra of atoms, molecules, and condensed media that involve the use of laser light. The most attention will be given to the laser spectroscopy of atoms.

As we already noted, the most important obstacle in the path of the experimental solution of the problems of optical spectroscopy is the Doppler broadening of the spectrum lines. This broadening limits the resolving

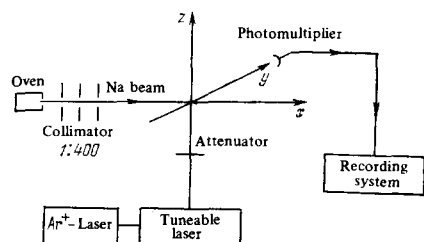


FIG. 6. Block diagram of equipment for a laser-excited atomic beam experiment.

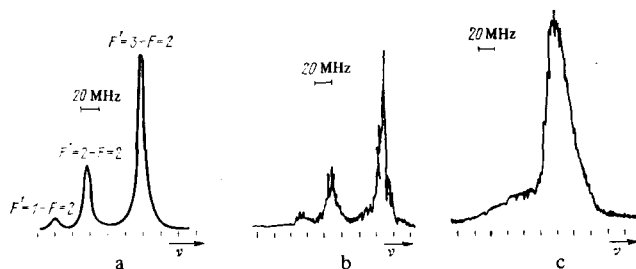


FIG. 7. Hyperfine structure of the $\text{Na } 3^2P_{3/2}-3^2S_{1/2}$ ($F=2$) transition (D_2 line) as calculated for the natural line widths (a) and recorded experimentally at low intensities of the exciting laser beam (b) and at an exciting-beam intensity of several mW/mm^2 (c).

power of the traditional methods, in which the contours of the spectrum lines, i.e., the frequency dependences of the emission (or absorption) intensity, are investigated in some way or other.

The methods of high resolution laser spectroscopy discussed below are closely related to classical spectroscopy, since here, too, one usually investigates line contours; here, however, the limiting resolution is not determined by the Doppler broadening, but by the natural line width. The high resolution is achieved by so arranging the experimental conditions that only atoms having a definite velocity component in a specified direction contribute to the observed effects.

A. Laser excitation of an atomic beam

The technique most closely related to traditional optical methods is to use a laser to excite an atomic beam^[27] (Fig. 6). This method differs from the classical method in that the fluorescence of the beam atoms is excited by a frequency tuneable practically monochromatic (frequency spread ~ 7 MHz) laser beam. Thanks to the use of an excitation source with a narrow frequency spread and controllable frequency, it is no longer necessary to include a Fabry-Perot interferometer in the observation channel. The recorded signal is the integral fluorescence power as a function of frequency. In this case we have the simplest conditions for the observation of both the absorption and fluorescence spectra, and the signal strength depends in a simple linear manner on the laser-beam power. The observed line width at low laser powers is close to the natural width. Moreover, there are no pressure shifts. The use of this technique to solve spectroscopic problems is facilitated by the fact that at low laser powers, the intensities of the investigated lines are proportional to the oscillator strengths. It is important to emphasize this, since in the nonlinear techniques considered later (saturation and two-photon absorption) the intensities are proportional to the squares of the oscillator strengths. However, the use of this method brings its own difficulties: For example, the beams must be highly collimated for optical recording of the signal, and limitation of the laser-beam power leads to recording difficulties.

As an example of the high resolution attainable by this method, Fig. 7 shows the structure of the $\text{Na } 3^2P_{3/2}$

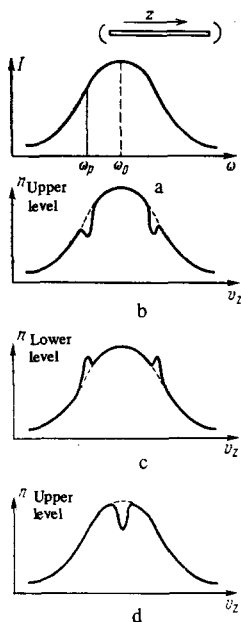


FIG. 8. Scheme illustrating the production of saturation resonances in a laser.

term as revealed by examination of the $3^2P_{3/2}-3^2S_{1/2}$ ($F=2$) transition. The experimental lines are about 15 MHz wide (Fig. 7, b). Figure 7, c shows what happens when the power of the optical-pumping laser beam is increased. A detailed discussion of the atomic beam method with laser excitation will be found in a review article by Jacquinet.^[28]

B. Saturated absorption spectroscopy

Let us briefly consider the physical idea underlying saturated absorption spectroscopy. A detailed theoretical treatment will be found in other review articles.^[4,5]

In saturated absorption spectroscopy one uses two light beams: a saturating beam, which "prepares" the set of atoms having a definite velocity component in the direction of the light field, and a probe beam, which analyzes this set of atoms.

It is convenient to begin our discussion of the effect with the processes that take place in a laser. The standing wave of the laser field in the cavity can be expressed as the sum of two oppositely directed traveling waves of the same frequency. If the profile of the active line of the working substance is not uniform (Doppler broadened because of the motion of the atoms), only those atoms will interact resonantly with the laser field whose velocities satisfy the equation $\omega_p = \omega_0(1 - n \cdot v/c)$, where ω_p is the proper frequency of the cavity, ω_0 is the frequency of the atomic transition, and n is a unit vector normal to the laser wave front (Fig. 8, a).

One of the waves (the one traveling in the direction of the z axis) interacts with atoms having negative velocity components v_x , and the other, with atoms having positive v_x . Thus, the laser field interacts with two groups of atoms characterized by opposite signs of v_x and burns two "holes" (Bennett dips) in the contour of the active line (Fig. 8, b) at equal distances from the center of the line.^[29] An excess of atoms in the lower level of the active transition having these values of v_x

will obviously be produced—"ears" will appear on the velocity distribution of these atoms (Fig. 8, c). When the resonant frequency of the cavity is adjusted to the center of the active line, both waves will interact with the same atoms (those for which $v_x = 0$) and the two Bennett dips will reduce to a single dip at the center of the line (Fig. 8, d). The width of this dip is determined by the natural width of the line corresponding to the given transition (in general, as broadened by collisions and by the action of the field power) and may be several orders of magnitude smaller than the Doppler width.

Detailed experimental studies of Bennett dips^[30-32] were published several years after the dips were discovered, and the use of Bennett dips in high resolution spectroscopy was proposed.^[33,34] Spontaneous emission at 6368 Å from the $3s_2$ laser level was investigated in^[32] (generation took place at $\lambda = 3.39 \mu\text{m}$ on the $3s_2-3p_4$ transition) and a Bennett dip was observed at the center of the line contour. In^[30,31] spontaneous emission from the $2p_4$ lower laser level was analyzed (generation took place at $\lambda = 1.15 \mu\text{m}$ on the $2s_2-2p_4$ transition) and "ears" were observed on the Doppler broadened line; moreover, saturation resonances were first used to determine the isotopic shift of Ne lines in^[31]. More careful recording of the line structure in^[35] made it possible to detect the asymmetry of the saturation resonances associated with the correlation between stimulated and spontaneous emission of photons.

In all of these experiments, the line contours were recorded with a Fabry-Perot interferometer and the spontaneous emission propagating along the laser beam or at a small angle to it was analyzed. These studies were further developed in^[36-38]. A beam of $1.15 \mu\text{m}$ radiation (analyzing beam) from a short frequency-tuneable He-Ne laser generating at 6328 Å (saturating field). The strong 6328 Å saturating field led to the formation of "ears" (Fig. 9) on the velocity distribution of the Ne atoms in the $2p_4$ state, as a result of which the amplification of the weak $1.15 \mu\text{m}$ probe beam decreased. The intensity of the transmitted infrared radiation was recorded as a function of its frequency, and this reflected the shape of the Bennett dips.

The use of absorption cells made it possible to employ low pressure discharges and thereby to avoid the

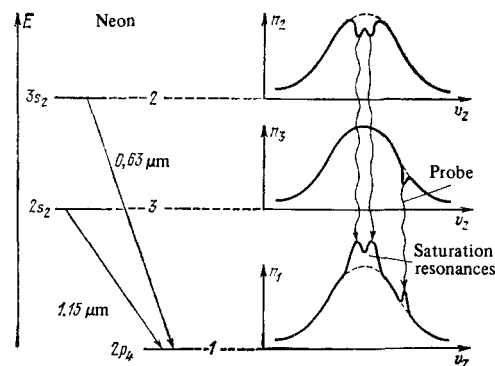


FIG. 9. Coupled transitions in Ne and a scheme illustrating the probing of saturation resonances.

pressure broadening of the resonances. On introducing an absorption cell into the laser cavity, a narrow peak appeared on the frequency distribution of the output power of the laser. The causes for the appearance of this peak are similar to those that lead to the production of the Lamb dip. Such a resonance was first observed experimentally in^[39,40], in which an He-Ne laser generating at 6328 Å was used with an absorption cell containing Ne²⁰. The width of the peak varied in the range ~15–35 MHz, depending on the experimental conditions. In^[41], a resonance of width of the order of 0.1–0.3 MHz was observed on putting an absorption cell filled with methane into the cavity of an He-Ne laser generating at 3.39 μm. It was suggested in^[42] that resonance saturation be used for selfstabilization of a laser frequency, and higher frequency stability and reproducibility was achieved^[43] than with the usual practice of using the Lamb dip for laser frequency stabilization.

The range of problems that can be solved by experiments of this type is limited by the laser media. The range of problems accessible to study by saturated absorption spectroscopy can be considerably extended by using tuneable lasers. In^[44] the authors investigated the structure of the sodium resonance lines at $\lambda_1 = 5896$ Å and $\lambda_2 = 5890$ Å by saturated absorption spectroscopy (in the foreign literature this technique is frequently called the Lamb dip method), using a tuneable pulsed dye laser. The experimental setup is depicted in Fig. 10. Two light beams (the probe and saturating beams) of the same frequency but differing greatly in intensity (0.5 and 50 mW) propagate in opposite directions through a cell containing sodium vapor, and the change in the intensity of the weak probe beam due to the presence of the strong saturating beam is recorded. A saturation resonance is observed only when the probe and saturating beams interact with the same atoms, whose velocities are perpendicular to the light beams, i. e., when the laser frequency is tuned to the center of the atomic transition.

A laser containing a 20 : 1 mixture of rhodamine 6G and rhodamine B and pumped with a nitrogen laser was used in the experiments. The width of the laser radiation was reduced from 300 to 7 MHz with the aid of a piezoelectric Fabry-Perot interferometer. The laser pulses were 30 nsec long and the pulse rate was 100 sec⁻¹.

The intensity of the probe beam was compared with

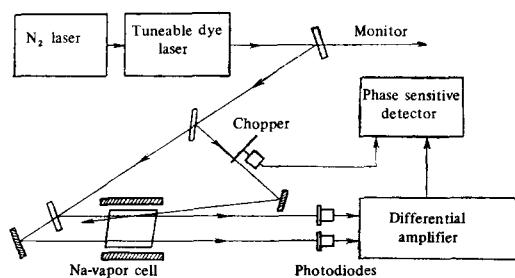


FIG. 10. Experimental setup for study of the fine structure of sodium lines by saturated absorption spectroscopy.

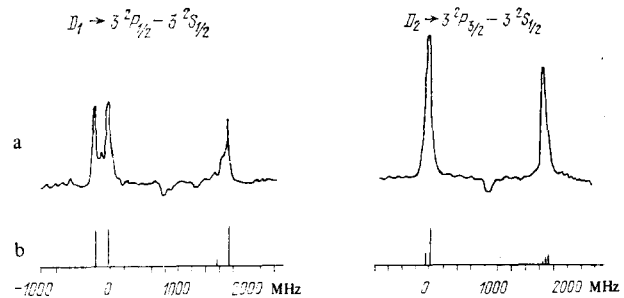


FIG. 11. Experimental recordings of saturated absorption signals for the Na $3^2P_{3/2}$ and $3^2P_{1/2}$ states (a) and the theoretical structures of the lines (b).

that of a second probe beam which traversed a path of the same length through the sodium cell but did not cross the saturating beam. This avoided effects due to the fluctuation of the laser field amplitude.

Figure 11 shows the HFS of the sodium *D* lines. The splitting of the close components (192 MHz) represents the HFS of the $3^2P_{1/2}$ level, while the 1772 MHz splitting represents the HF splitting of the $3^2S_{1/2}$ ground state. As is evident from the figure, additional components lying halfway between HFS components having a common level were detected in the experiment. These arise from the fact that the velocity components of some atoms are such that the saturating wave is in resonance with one of the HF components while the probe beam is in resonance with the other. The additional signal between components having a common upper level is negative; this is due to the presence of optical pumping that populates the HF component of the ground state and therefore leads to additional absorption of the probe beam. In the best case, the width of a component as measured in this experiment amounted to 40 ± 4 MHz. This means that the spectrum lines were appreciably broadened (the natural width does not exceed 10 MHz), owing to the finite width of the laser line and to the fact that the saturating and probe beams were not exactly parallel. For this reason the authors were unable to resolve the HFS of the $3^2P_{3/2}$ state, as is evident from Fig. 11. It is interesting that in studying the dependence of the widths of the saturation resonances on the probe beam delay time with a buffer gas in the cell, it was possible to observe the effect of velocity changes due to collisions on the resonance widths. It is important that one can distinguish the effects of collisions leading to velocity changes from those of line broadening collisions in experiments of this type.

The capabilities of saturated absorption spectroscopy are clearly demonstrated in^[45,46]; in these studies the authors succeeded in resolving the fine structure components of the H_α line of hydrogen (the red Balmer line) and the D_α line of deuterium and in determining the Lamb shift with a precision unprecedented in optical measurements (Fig. 12). In this same experiment the Rydberg constant was determined with an order of magnitude higher precision than in previous measurements, and new precise values were obtained for the isotopic shift between H_α and D_α . The saturation resonance signals from the fine structure components of the hydrogen

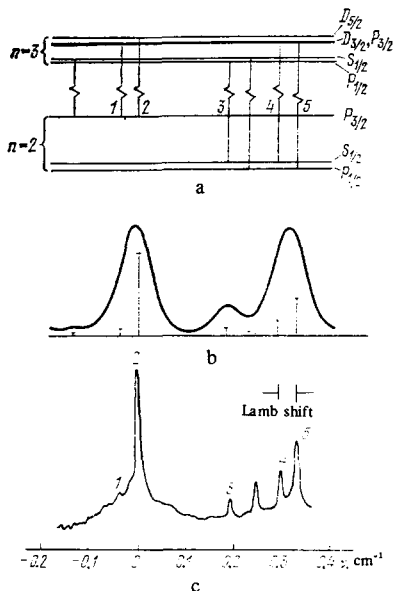


FIG. 12. Fine structure of the deuterium D_α line (a), the D_α line from a cold deuterium discharge showing the fine structure and the relative transition probabilities^[53] (b), and saturated absorption signals showing the fine structure (c).

and deuterium lines were detected in the same way as in the experiment on the HF components of the sodium lines described above. The only difference was that a dc discharge was maintained in the absorption cell; this excited the hydrogen and deuterium atoms to the $n=2$ state, and the absorption from this level was measured by saturated absorption spectroscopy. A recording of the fine structure components of the D_α line is shown in Fig. 12, c, in which the excellent resolution of the Lamb shift is clearly evident. The strongest component (the $3D_{5/2}-2P_{3/2}$ transition) was used to determine the Rydberg constant. To determine the precise wavelength for this transition the wavelength of the tuneable laser radiation was measured with a stabilized Fabry-Perot interferometer. The results shown in Table I illustrate the high precision that can be achieved in saturated absorption spectroscopy measurements.

C. Two-photon absorption laser spectroscopy

The two-photon excitation method proposed in 1970 by Chebotaev^[47] is perhaps the most promising method of high resolution laser spectroscopy. To clarify the idea behind this very elegant method let us discuss the following thought experiment. Let the cell K (Fig. 13,

a) contain atoms of type A . In the level scheme for these atoms (Fig. 13, b) let level 1 be the ground state and let the transitions $2-1$ and $3-2$ be allowed by the selection rules for electric dipole radiation. Then the electric dipole transition $3-1$ is obviously forbidden. Now let two beams obtained from the same laser, whose frequency ω_L can be varied in the vicinity of $\omega_0/2$ (ω_0 being the frequency of the forbidden $3-1$ transition), propagate in opposite directions through the cell K . If the laser radiation is intense enough and if the angular momenta of levels 1 and 3 are equal or differ by 2 units, we may expect some of the atoms A to be excited from state 1 to state 2 as a result of two-photon absorption. As a measure of the intensity of this nonlinear effect we may take, for example, the intensity of the subsequent spontaneous emission from the $3-2$ transition.

Now let us discuss what may be expected concerning the dependence of the intensity of this spontaneous radiation on the laser frequency ω_L . Let us first consider the subensemble A_0 of atoms consisting of those for which the component v_z of the velocity of thermal motion in the direction of the exciting light is close to zero. It is clear that the contribution from this subensemble to the observed dependence will be a Lorentz curve of which $\gamma_3=1/\tau_3$, where τ_3 is the lifetime of level 3 with respect to all decay channels. The peak of this curve will come at the two-photon absorption resonance frequency $\omega_L=\omega_0/2$. Now let us consider the rest of the atoms. We consider an arbitrary atom for which v_z differs from zero and follow it in detail. In doing this it is convenient to use a reference system moving with velocity v_z along the z axis of the laboratory system (we choose the z axis of the laboratory system so that $v_z > 0$). In this system the level scheme for atom A is still the same as that shown in Fig. 13, b since it can always be assumed that the rms velocity u of thermal motion is much lower than the velocity c of light. Let the laser be tuned to two-photon resonance with the subensemble A_0 . Then in the selected reference system, the beam traveling in the positive z direction (the direction of the velocity component v_z of the selected atom in the lab system) will have the frequency $(1/2)\omega_0(1-v_z/c)$, while the opposite beam will have the frequency $(1/2)\omega_0(1+v_z/c)$. The sum of the energies of two photons taken one from each of the beams will then be $\hbar\omega_0$, so that the selected atom (and with it, all the atoms, since v_z was arbitrary) will participate in the two-photon resonance absorption. If the resonance condition is violated for stationary atoms ($v_z=0$) it will be violated for all the atoms. Hence we may expect the

TABLE I.

	H_α	D_α
Lamb shift	1052.7 (1.7) MHz	
Vacuum wavelength ($3D_{5/2}-2P_{3/2}$)	15233.07021 (9) cm^{-1}	15237.21538 (8) cm^{-1}
Isotopic shift		4.14517 (12) cm^{-1}
Rydberg constant	109737.3130 (6) cm^{-1} 109737.3143 (10) cm^{-1}	109737.3150 (6) cm^{-1}

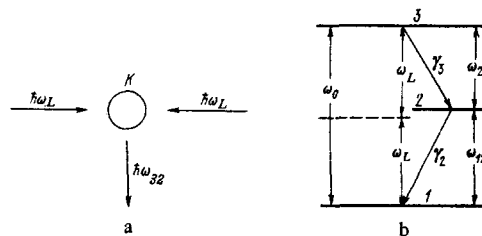


FIG. 13. Illustrating the two-photon excitation method.

dependence of the intensity of the spontaneous emission from the 3-2 transition on the frequency ω_L in two-photon absorption from opposing beams to have the Lorentz shape with the width γ_3 .

Now let us consider two-photon absorption from a single beam. In this process the radiation tuned to the two-photon resonance for the subensemble A_0 will be weakly absorbed by moving atoms since $2(1/2)\hbar\omega_0(1 \pm v_x/c) \neq \hbar\omega_0$. On the other hand, radiation detuned from the two-photon resonance for stationary atoms will be resonantly absorbed by those atoms whose velocity component v_x satisfies the condition $v_x = \pm c(2\omega_L - \omega_0)/2\omega_L > 0$. Here the two signs correspond to the two possible directions of propagation of the beam with respect to the velocity component v_x of the atom. From this it is clear that the narrow Lorentz peak for two-photon absorption from opposing beams must be observed against the background of the Doppler broadened absorption from a single beam.

The qualitative considerations presented here constitute a fairly adequate commentary on the theoretical two-photon absorption profile derived in^[47] for the limiting case $\omega_0 u/c \gg \gamma_3$:

$$\langle P(2\omega_L) \rangle = \frac{|V_{21}|^2 |V_{32}|^2 / \omega_0}{8\hbar^4 (\omega_{21} - \omega_L)^2} \left(\frac{1}{2K_L u} e^{-\Omega^2 / (2K_L u)^2} + \frac{2\gamma_3}{\gamma_3^2 + \Omega^2} \right);$$

here V_{21} and V_{32} are matrix elements of the operator for the interaction of the atom with the laser field, $K_L = \omega_L/c$, and $\Omega = |\omega_0 - 2\omega_L|$ is the detuning of the laser from the two-photon resonance with stationary atoms. The formula contains information regarding conditions that would favor the observation of the effect. These conditions have already been discussed in part (the 3-2 and 2-1 transitions should be allowed). Here we note that the smaller the difference between $\omega_0/2$ and ω_{21} , the lower the power required for observing the effect. It is interesting that the two-photon absorption profile looks simpler than one with stronger Doppler broadening. Actually, according to the formula the ratio of the height of the Doppler peak to the height of its Gaussian pedestal is $4K_L u / \sqrt{\pi} \gamma_3$ and increases with increase in the rms thermal velocity u .

In connection with the availability of tuneable lasers with very narrow lines and good precision in setting the frequency, several experimental studies that il-

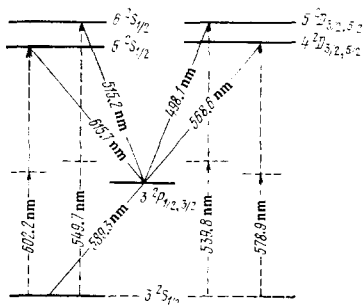


FIG. 14. Na terms investigated in^[48-51] by the two-photon excitation method.

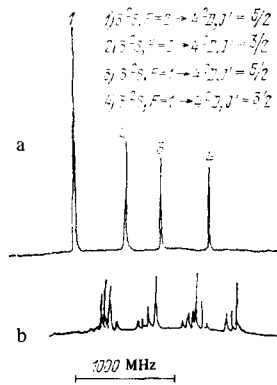


FIG. 15. Structure of the $3^2S_{1/2} - 4^2D$ two-photon transition in sodium^[48]. a—in zero magnetic field, b—the σ^+ components of the magnetic structure in a 170 G field.

lustrate the capabilities of the method have been published very recently.^[48-51] The principal results of these studies were reported at the Fourth International Conference on Atomic Physics at Heidelberg.^[53] The measurements were made on sodium vapor excited by two opposing beams from a tuneable dye laser. Both continuous and pulsed lasers were used. The laser power required for the experiment proved not to be too high. For example, in^[51] two-photon absorption on the $3^2S(F=2) - 4^2D_{5/2}$ transition was reliably detected with a 30 mW exciting beam concentrated on an area 40 μm in diameter. The spontaneous emission accompanying the decay of the excited level was used to detect the two-photon absorption. Ordinary glass filters or interference filters were used to isolate the spontaneous emission from the scattered laser light.

Figure 14 shows the Na terms examined in these studies and indicates the laser-beam wavelengths corresponding to the two-photon resonances. Figure 15, a shows the structure of the $3^2S_{1/2} - 4^2D$ two-photon transition obtained in^[48]. The observed peaks are about 12 MHz wide. Figure 15, b shows the components of the magnetic structure of this transition in a 170 G field, and the same structure in a 9860 G field is shown on a larger scale in Fig. 16. The information obtained in these studies is presented systematically in Table II.

On analyzing the results of these first studies one can see a number of advantages of the two-photon excitation method. The main advantage of the method over saturated absorption spectroscopy is that all the atoms,

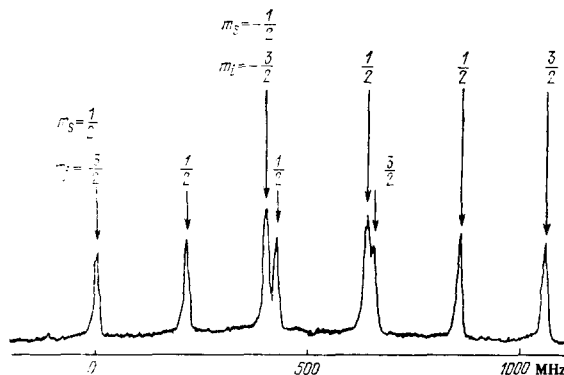


FIG. 16. Structure of the σ^+ components of the $3^2S_{1/2} - 4^2D$ transition in sodium in a 9860 G field.^[48]

TABLE II.

Na term	Laser wavelength λ_L , nm	Fine (D) Hyperfine (S) splitting, MHz	Hyperfine structure constant A, MHz
$5^2S_{1/2}$	602.2	156 ± 10	78 ± 5
$6^2S_{1/2}$	549.7	78 ± 6	39 ± 3
4^2D	578.9	1025 ± 6 ⁵⁰ , 1035 ± 15 ⁵¹	
5^2D	539.8	618 ± 12	

not just those that have a zero velocity component in the direction of the laser beam, take part in forming narrow peaks free of Doppler broadening. This tends to improve the signal to noise ratio. Finally, the two-photon excitation method can be used to investigate high-lying levels, on which information is most lacking at present.

4. CONCLUSION

It is interesting to compare the capabilities of the methods under consideration. Such a comparison is made somewhat difficult by the fact that the data obtained by the two methods (laser spectroscopy and the level crossing method) differ widely. In the level crossing method one investigates a definite atomic level, while laser spectroscopy is concerned with transitions between levels, which, as was pointed out, enables one to determine isotopic shifts. Hence we shall not consider the differences between these methods but shall compare related information obtained by both methods. For example, the level crossing method can be used to determine the hyperfine structure constants A and B , as well as the lifetime, of the investigated level. Similar information can be obtained by analyzing a spectrum recorded by methods of laser spectroscopy.

It seems possible to compare the accuracy in determining the HFS constants by the two methods on the basis of available data. The values obtained for A and B for the Na $3^3P_{3/2}$ state by laser excitation of an atomic beam^[27,52] are in good agreement with earlier data on this level obtained by methods involving interference of atomic states (see, e.g., the table in^[52]). The error in determining these constants is about twice the error achieved in^[52], where the Na $3^2P_{3/2}$ state was investigated by the level crossing method with time resolution.

We note once more that the hyperfine structure of the Na $3^2P_{3/2}$ state could not be resolved at all by saturated absorption spectroscopy.^[44]

As regards the accuracy in determining the magnetic dipole interaction constant for high-lying alkali-metal levels, we note that an analysis of the results given in^[25] and^[49] shows that the error in determining this constant by the level crossing method is about half the error obtained using laser spectroscopy with two-photon excitation.

It is not possible to compare the accuracy of the two methods in determining the lifetimes of levels at present because the necessary data are not given in existing papers on laser spectroscopy. Generally

speaking, the extraction of information on lifetimes from the shapes of lines recorded by these methods is complicated by the finite width of the laser line and a number of secondary processes.

On comparing the level crossing and high-resolution laser spectroscopy methods, we cannot fail to note the main difficulty besetting the latter: the necessity of using unique tuneable lasers with sufficiently narrow lines. We may expect, however, that with progress in the design and construction of tuneable lasers, the laser spectroscopy methods will eventually become simpler and no less accurate than the level crossing method.

The authors are grateful to M. P. Chaika for a number of interesting and valuable discussions.

- ¹M. P. Chaika, Interferentsiya vyrozhdennykh atomnykh sostoyanii (Interference of degenerate atomic states), L., Izd-vo Leningr. un-ta, 1975.
- ²N. I. Kaliteevskii, Zh. Prikl. Spektrosk. 19, 166 (1973).
- ³Atomic Physics-4 (Fourth International Conference on Atomic Physics, Heidelberg, 1974), Plenum, N. Y., 1975.
- ⁴V. S. Letokhov and V. P. Chebotaev, Printsipy nelineinoi lazernoï spektroskopii (Principles of nonlinear laser spectroscopy), M., Nauka, 1975.
- ⁵I. M. Beterov and R. I. Sokolovskii, Usp. Fiz. Nauk 110, 169 (1973) [Sov. Phys. Usp. 16, 339 (1973)].
- ⁶V. S. Litokhov and V. P. Chebotaev, Usp. Fiz. Nauk. 113, 386 (1974) [Sov. Phys. Usp. 17, 467 (1975)].
- ⁷A. L. Mashinskii and M. P. Chaika, Opt. Spektrosk. 28, 1093 (1970). [Opt. Spectrosc. 28, 589 (1970)].
- ⁸L. Volnikova, V. Grigor'eva, G. Khvostenko, and M. Chaika, Opt. Spektrosk. 30, 170 (1971) [Opt. Spectrosc. 30, 88 (1971)].
- ⁹V. N. Grigor'eva, G. I. Khvostenko, and M. P. Chaika, Opt. Spektrosk. 34, 1224 (1973) [Opt. Spectrosc. 34, 712 (1973)].
- ¹⁰V. Grigor'eva, Vestn. LGU, ser. "Fizika, khimiya", No. 16, 44 (1973).
- ¹¹S. Chang, R. Gupta, and W. Happer, Phys. Rev. Lett. 27, 1036 (1971); R. Gupta, S. Chang, C. Tai, and W. Happer, *ibid.* 29, 695 (1972).
- ¹²Y. Archambault, J. P. Descourbes, M. Priou, A. Omont, and J. C. Pélbay-Peyroula, J. Phys. Radium 21, 677 (1960).
- ¹³E. L. Al'tman, Opt. Spektrosk. 28, 1029 [Opt. Spectrosc. 28, 556 (1970)].
- ¹⁴T. Krupenikova and M. Chaika, Opt. Spektrosk. 20, 1088 (1966) [Opt. Spectrosc. 20, 604 (1966)].
- ¹⁵T. Hänsch and P. Toschek, Phys. Lett. 20, 273 (1966).
- ¹⁶B. Decomps and M. Dumont, C. R. Acad. Sci. (Paris) 262, 1004 (1966).
- ¹⁷G. Todorov, Candidate Dissertation, NIFI LGU, L., 1973.
- ¹⁸E. Kotlikov, G. Todorov, and M. Chaika, Opt. Spektrosk. 30, 185 (1971) [Opt. Spectrosc. 30, 99 (1971)].
- ¹⁹G. Todorov and M. Chaika, Opt. Spektrosk. 23, 826 (1967) [Opt. Spectrosc. 23, 449 (1967)].
- ²⁰E. N. Kotlikov, Opt. Spektrosk. 34, 203 (1973) [Opt. Spectrosc. 34, 114 (1973)].
- ²¹K. Boyarskii and E. Kotlikov, Kvant. Elektron. 2, 23 (1975) [Sov. J. Quantum Electron. 5, 10].
- ²²S. A. Kazantsev, A. Kisling, and M. P. Chaika, Opt. Spektrosk. 34, 1227 (1973); 36, 1030 (1974) [Opt. Spectrosc. 34, 714 (1973); 36, 606 (1974)].
- ²³M. P. Chaika, Opt. Spektrosk. 30, 822 (1974) [Opt. Spectrosc. 30, 443 (1974)].
- ²⁴Kh. V. Kallas and M. P. Chaika, Opt. Spektrosk. 27, 694 (1969) [Opt. Spectrosc. 27, 376 (1969)].

- ²⁵S. Svanberg, P. Tsekeris, and W. Happer, Phys. Rev. Lett. **30**, 817 (1973).
- ²⁶S. Svanberg and G. Belin, J. Phys. **B7**, L82 (1974).
- ²⁷W. Lange, J. Luther, *et al.*, Opt. Commun. **8**, 157 (1973).
- ²⁸P. Jacquinot, Ref. 3, p. 615.
- ²⁹W. R. Bennett Jr., Phys. Rev. **126**, 580 (1962).
- ³⁰W. G. Schweitzer Jr., M. M. Birky, and J. A. White, J. Opt. Soc. Am. **57**, 1226 (1967).
- ³¹R. H. Cordover, P. A. Bonczyk, and A. Javan, Phys. Rev. Lett. **18**, 730 (1967).
- ³²R. Bennett Jr., V. P. Chebotayev, and J. W. Knutson, in Fifth International Conference on the Physics of Electron and Atomic Collisions, Abstracts of Papers, L., Nauka, 1967.
- ³³A. Javan, in Quantum Optics and Electronics, Gordon and Breach, N. Y., 1965, p. 383.
- ³⁴J. A. White, J. Opt. Soc. Am. **55**, 1439 (1965).
- ³⁵Helen K. Holt, Phys. Rev. Lett. **20**, 410 (1968).
- ³⁶T. Hänsch and P. Toschek, IEEE J. Quantum Electron. **QE-4**, 467 (1968).
- ³⁷T. Hänsch and P. Toschek, IEEE J. Quantum Electron. **QE-4**, 530 (1968).
- ³⁸T. Hänsch and P. Toschek, IEEE J. Quantum Electron. **QE-5**, 61 (1969).
- ³⁹P. H. Lee and M. L. Skolnick, Appl. Phys. Lett. **10**, 303 (1967).
- ⁴⁰V. N. Lisitsyn and V. P. Chebotayev, Zh. Eksp. Teor. Fiz. **54**, 419 (1968) [Sov. Phys. JETP **27**, 227 (1968)].
- ⁴¹R. L. Barger and J. L. Hall, Phys. Rev. Lett. **22**, 4 (1968).
- ⁴²V. S. Letokhov, Pis'ma Zh. Eksp. Teor. Fiz. **6**, 597 (1967) [JETP Lett. **6**, 101 (1967)].
- ⁴³S. N. Bagaev, Y. D. Kolonnikov, V. N. Lisitsyn, and V. P. Chebotayev, IEEE J. Quantum Electron. **QE-4**, 868 (1968).
- ⁴⁴T. W. Hänsch, I. S. Shain, and A. L. Schawlow, Phys. Rev. Lett. **27**, 707 (1971).
- ⁴⁵T. W. Hänsch, I. S. Shain, and A. L. Schawlow, Nature (Lond.) Phys. Sci. **235ps**, 63 (1972).
- ⁴⁶T. W. Hänsch, M. N. Nayfeh, *et al.*, Phys. Rev. Lett. **32**, 1336 (1974).
- ⁴⁷L. S. Vasilenko, V. P. Chebotayev, and A. V. Shishaev, Pis'ma Zh. Eksp. Teor. Fiz. **12**, 161 (1970) [JETP Lett. **12**, 113 (1970)].
- ⁴⁸F. Biraben, B. Cagnac, and G. Grynberg, Phys. Rev. Lett. **32**, 643 (1974).
- ⁴⁹M. D. Levenson and N. Bloembergen, Phys. Rev. Lett. **32**, 645 (1974).
- ⁵⁰D. Pritchard, J. Apt, and T. W. Ducas, Phys. Rev. Lett. **32**, 641 (1974).
- ⁵¹T. W. Hänsch, K. C. Harvey, *et al.*, Opt. Commun. **11**, 50 (1974).
- ⁵²J. S. Deech, P. Hannaford, and G. W. Series, J. Phys. **B7**, 1131 (1974).
- ⁵³B. P. Kibble, W. R. C. Rowley, *et al.*, J. Phys. **B6**, 1079 (1973).

Translated by E. Brunner